ELSEVIER
Thermochimica Acta 391 (2002) 87–95
thermochimica acta
www.elsevier.com/locate/tca

Mathematical modeling of the thermal system of modulated temperature differential scanning calorimeter

Yasuo Saruyama[a,*], Guy Van Assche[b,1]

[a]Department of Polymer Science and Engineering, Kyoto Institute of Technology, Matsugasaki, Sakyo-ku, Kyoto 606-8585, Japan
[b]Venture Laboratory, Kyoto Institute of Technology, Matsugasaki, Sakyo-ku, Kyoto 606-8585, Japan

Received 31 August 2001; received in revised form 28 January 2002; accepted 31 January 2002

Abstract

Mathematical models for the thermal system of the modulated temperature differential scanning calorimeter were studied paying attention to the high frequency region. We took account of the thermal resistance between the pan and the base plate, deviation from the symmetric thermal system and time lag between the temperature of the base plate just below the pan and the measured temperature. Two types of equations for data analysis using only the temperature difference between the sample and reference sides are presented. The upper limit of the sample thickness for meaningful measurement was critically studied using thermal diffusion equation with proper boundary conditions. Results of the calculation were in good agreement with experimental results by the light heating modulated temperature differential scanning calorimetry (LMDSC).

Keywords: Modulated temperature DSC; Mathematical models; High frequency; Asymmetric system; Frequency dependence

1. Introduction

Modulated temperature differential scanning calorimetry (MTDSC) has been used as a new and useful technique to study thermal properties of materials. The conventional differential scanning calorimetry (DSC) instrument can be used as MTDSC by replacing the software for machine operation and data processing. A new method of data analysis to calculate the heat capacity was proposed by Wunderlich et al. [1]. Wunderlich's method was used in the data processing software of the commercial instruments. Wunderlich's equation is based on the typical model for the conventional DSC instrument regarding the sample material, the pan, the lid and the detector as one body without temperature distribution in it. Hatta [2] proposed an improved method of experiment and data analysis, which can be used by the commercial machine and software, taking account of the thermal resistance between the pan and the base plate.

Saruyama and coworkers [3,4] constructed another type of MTDSC, called light heating modulated temperature differential scanning calorimeter (LMDSC), using light energy to generate temperature modulation. In LMDSC the light with modulated intensity irradiates the upper surface of the sample cell directly. Therefore, LMDSC can be operated at higher frequencies (0.01–1 Hz) than typical commercial instruments

---

[*] Corresponding author. Fax: +81-75-724-7738.
E-mail address: saruyama@ipc.kit.ac.jp (Y. Saruyama).

[1] Present address: Department of Physical Chemistry and Polymer Science, Free University of Brussels (VUB), Pleinlaan 2, B-1050 Brussels, Belgium.

PII: S0040-6031(02)00166-1

(<0.1 Hz). As frequency becomes higher the model used for Wunderlich's equation becomes insufficient because the time required for heat exchange between, e.g. the pan and the base plate becomes comparable to the modulation period. Saruyama [5,6] has used different methods from Wunderlich's equation to analyze the data obtained by LMDSC. Saruyama's equations were successfully used but systematic studies starting from proper models have not been made and limitation of applicability has not been investigated in detail.

In this work, we carried out detailed calculation to elucidate the mathematical relationship between the heat capacity of the sample and the observed signal at high frequencies. In this paper, two models are studied. Model 1 that is similar to the model used by Wunderlich is studied for comparison with model 2. In model 2, we take account of the thermal resistance between the pan and the base plate and the time lag between the temperature of the base plate just below the pan and the measured temperature. In both models, we do not assume that the thermal system composed of the sample chamber, the base plate and the pans is symmetric for the sample and reference sides. Sample thickness that becomes critical at high frequencies is investigated on the basis of the model 2. Results from the model 2 are compared with experimental results at frequencies higher than 0.1 Hz using LMDSC. Methods of data analysis suitable for the model 2 are presented.

2. Models and basic equations

2.1. Model 1

Fig. 1 shows a simple model in which the sample or reference material, the pan, the lid and the detector are considered as one body without temperature distribution in it. The "detector" means the area of the base plate just below the pan. "Sample (or reference) material" means the integrated "one body" in this section. We take account of heat exchange between the sample/reference material and the wall of the sample chamber and between the sample and reference materials. The basic equations for model 1 are given as follows:

$$i\omega C_s T_s = L - M_1 T_s + M_2 T_r - B_1 T_s + B_2 T_b \qquad (1)$$

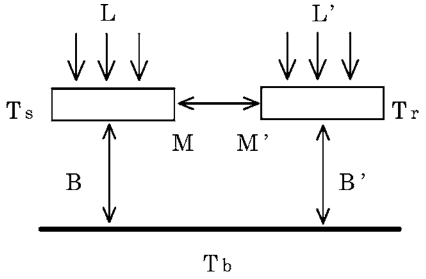

Fig. 1. Model 1 of the thermal system of MTDSC. The sample material, the pan, the lid and the detector are regarded as one body without temperature distribution.

$$i\omega C_r T_r = L' - M'_1 T_r + M'_2 T_s - B'_1 T_r + B'_2 T_b \qquad (2)$$

where C_s and C_r are the heat capacity of the sample and reference materials, respectively. In this paper, the quasi-isothermal condition is considered. Therefore, only the periodic temperature change around a fixed value is considered. We use expression by complex number for the periodic temperature change such as $A \exp(i\omega t)$, where A, ω and t are complex amplitude, angular frequency of the modulation and time, respectively. T_s, T_r and T_b are the complex amplitudes of the temperatures of the sample material, the reference material and the heat bath (the wall of the sample chamber), respectively. Time derivative is replaced with $i\omega$ on the left-hand side of Eqs. (1) and (2). L and L' are the complex amplitudes of energy flow of the light irradiating the sample and reference materials in LMDSC, respectively. In the case of LMDSC T_b can be set to be 0 because the temperature of the wall of the sample chamber is not modulated by the light energy. On the other hand, L and L' are 0 in the commercial instruments. Accordingly, Eqs. (1) and (2) are applicable both to LMDSC and the commercial instruments.

The heat flow is assumed to be linear to the temperature change as explained later. We consider, e.g. heat flow into the sample material due to the temperature change in the reference material. Linearity means that the time dependence of the heat flow is expressed by $A \exp(i\omega t)$ and the complex amplitude A is given by a complex constant times T_r. This corresponds to the third term of the right-hand side of Eq. (1) in which the complex constant is written as M_2. Since M_2 is a complex number the initial phase of the heat flow is different from that of T_r. This phase difference expresses the delay of the heat flow after the temperature change. Similarly, M_1T_s of the second term expresses the heat flow out of the sample material due to the temperature change in the sample material. The coefficients M_1 and M_2 are not equal to each other. An example of calculation of such coefficients is given in Appendix B for equations presented later. Heat exchange between the sample material and the wall of the sample chamber is given by the terms of coefficients B_1 and B_2. Eq. (2) is for the reference side. Primed parameters are used in Eq. (2) because we take account of deviation from the symmetric thermal system.

Eqs. (1) and (2) can be solved and T_s and T_r are expressed as follows:

$$T_s = \frac{(L + B_2T_b)(i\omega C_r + M'_1 + B'_1) + (L' + B'_2T_b)M_2}{(i\omega C_s + M_1 + B_1)(i\omega C_r + M'_1 + B'_1) - M_2M'_2} \quad (3)$$

$$T_r = \frac{(L' + B'_2T_b)(i\omega C_s + M_1 + B_1) + (L + B_2T_b)M'_2}{(i\omega C_s + M_1 + B_1)(i\omega C_r + M'_1 + B'_1) - M_2M'_2} \quad (4)$$

Temperature difference $\Delta T = T_s - T_r$ and the ratio $\Delta T/T_s$ are given by the following equations:

$$\Delta T = \frac{1}{(i\omega(\Delta C + C_r) + M_1 + B_1)(i\omega C_r + M'_1 + B'_1) - M_2M'_2}\{-i\omega\Delta C(L' + B'_2T_b) + (L + B_1T_b)(i\omega C_r + M'_1 + B'_1 - M'_2) - (L' + B'_2T_b)(i\omega C_r + M_1 + B_1 - M_2)\} \quad (5)$$

$$\frac{\Delta T}{T_s} = \frac{1}{(L + B_2T_b)(i\omega C_r + M'_1 + B'_1) + (L' + B'_2T_b)M_2} \times \{-i\omega\Delta C(L' + B'_2T_b) + (L + B_1T_b) \times (i\omega C_r + M'_1 + B'_1 - M'_2) - (L' + B'_1T_b) \times (i\omega C_r + M_1 + B_1 - M_2)\} \quad (6)$$

where $\Delta C = C_s - C_r$. It should be noted that the left-hand side of Eq. (6) is not proportional to ΔC in contrast with Wunderlich's equation [1]. The proportionality holds when the thermal system is symmetric as assumed in the model used by Wunderlich.

2.2. Model 2

Hatta pointed out that perfect thermal contact between the pan and the base plate is too simplified in many cases [2]. Fig. 2 shows model 2 in which the thermal resistance between the pan and the base plate and time lag between the temperature change at the detector and the measured temperature are considered. The latter is necessary to be considered because the measuring point is at the bottom of a small dent at the center of the detector area. The sample or reference material, the pan and the lid are considered as one body without temperature distribution in it. The basic equations for the sample side of the model 2 are given as follows:

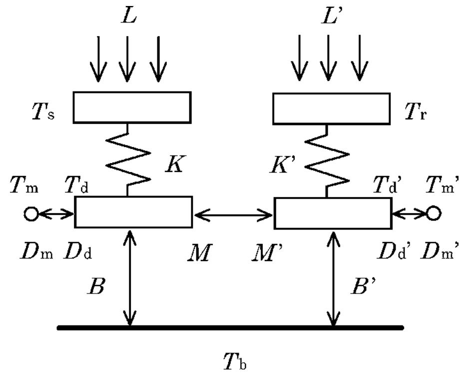

Fig. 2. Model 2 of the thermal system of MTDSC. Thermal resistance between the pan and the base plate, and time lag between the temperature of the base plate just below the pan and the measured temperature are taken into account.

$$i\omega C_sT_s = L - K(T_s - T_d) \quad (7)$$

$$i\omega C_dT_d = -K(T_d - T_s) - M_1T_d + M_2T'_d - B_1T_d + B_2T_b - D_{d1}T_d + D_{d2}T_m \quad (8)$$

$$i\omega C_mT_m = -D_{m1}T_m + D_{m2}T_d \quad (9)$$

The thermal resistance between the pan and the base plate is assumed to follow the Newton's law. K is the coefficient of the Newton's law. C_d and T_d are the heat capacity and the complex amplitude of the temperature of the detector, respectively.C_m and T_m are those of the measuring point. D_{d1}, D_{d2}, D_{m1} and D_{m2} are the coefficients for the heat exchange between the detector and the measuring point. $\Delta T = T_{\mathrm{m}} - T'_{\mathrm{m}}$ and $\Delta T/T_{\mathrm{m}}$ are given by the following equations:

$$\Delta T = \frac{(\lambda_{\mathrm{L}}L' + \lambda_{\mathrm{b}}T_{\mathrm{b}})\Delta C + \mu_{\mathrm{L}}L - \mu'_{\mathrm{L}}L' + \mu_{\mathrm{b}}T_{\mathrm{b}}}{v\Delta C + \xi} \tag{10}$$

$$\frac{\Delta T}{T_{\mathrm{m}}} = \frac{(\lambda_{\mathrm{L}}L' + \lambda_{\mathrm{b}}T_{\mathrm{b}})\Delta C + \mu_{\mathrm{L}}L - \mu'_{\mathrm{L}}L' + \mu_{\mathrm{b}}T_{\mathrm{b}}}{(\eta_{\mathrm{L}}L' + \eta_{\mathrm{b}}T_{\mathrm{b}})\Delta C + \zeta_{\mathrm{L}}L + \zeta'_{\mathrm{L}}L' + \zeta_{\mathrm{b}}T_{\mathrm{b}}} \tag{11}$$

Eqs. (10) and (11) show that the light energy and the heat flow from the wall of the sample chamber play the same role with each other even at the high frequencies where the thermal resistance between the pan and the base plate can not be neglected. Meaning of Greek letters in Eqs. (10) and (11) are explained in Appendix A. It should be noted that the Greek letter parameters are independent of the heat capacity of the sample. The denominator of the right-hand side of Eq. (11) includes the term of ΔC that dose not vanish if the system is symmetric. For quantitative measurement values of $(\mu_{\mathrm{L}}L - \mu'_{\mathrm{L}}L' + \mu_{\mathrm{b}}T_{\mathrm{b}})/(\lambda_{\mathrm{L}}L' + \lambda_{\mathrm{b}}T_{\mathrm{b}})$, $(\eta_{\mathrm{L}}L' + \eta_{\mathrm{b}}T_{\mathrm{b}})/(\lambda_{\mathrm{L}}L' + \lambda_{\mathrm{b}}T_{\mathrm{b}})$ and $(\varsigma_{\mathrm{L}}L - \varsigma'_{\mathrm{L}}L' + \varsigma_{\mathrm{b}}T_{\mathrm{b}})/(\lambda_{\mathrm{L}}L' + \lambda_{\mathrm{b}}T_{\mathrm{b}})$ have to be determined using standard materials. There is no advantage of data analysis using $\Delta T/T_{\mathrm{m}}$ in comparison with using only ΔT because the number of values to be determined using standard materials is same in Eqs. (10) and (11). This is an essential difference between the models 1 and 2. It should be noted that signal-to-noise ratio of ΔT is better than that of T_{m} since DC component of the temperature difference is much smaller than that of the sample temperature. From this viewpoint, data analysis using only ΔT is better than using $\Delta T/T_{\mathrm{m}}$.

Eq. (11) becomes the same form with Eq. (6) if the following condition is satisfied:

$$|i\omega\Delta C| \ll |i\omega C_{\mathrm{r}} + K| \tag{12}$$

In order to satisfy the condition (12) for a given K, the modulation frequency and/or ΔC have to be small.

3. Sample thickness

It is commonly noticed that the sample thickness has to be sufficiently thin. We studied the upper limit of the sample thickness for meaningful measurement starting from the thermal diffusion equation considering the proper boundary condition on the basis of the model 2. In order to take account of thermal diffusion in the sample the following equations are used instead of Eq. (7).

$$i\omega C_{\mathrm{l}}T_{\mathrm{l}} = L - S_1T_{\mathrm{l}} + S_2T_{\mathrm{p}} \tag{13}$$

$$i\omega C_{\mathrm{p}}T_{\mathrm{p}} = -S_1T_{\mathrm{p}} + S_2T_{\mathrm{l}} - K(T_{\mathrm{p}} - T_{\mathrm{d}}) \tag{14}$$

C_{l} and T_{l} are the heat capacity and the complex amplitude of the temperature modulation of the lid, respectively. C_{p} and T_{p} are those of the pan. Thermal diffusion in the sample is expressed by the terms of S_1 and S_2. From Eqs. (13) and (14) the following equation is deduced:

$$i\omega\left(\left(1 + \frac{R}{2}\right)\frac{2S_-}{i\omega} + C_{\mathrm{p}} + (1 + R)C_{\mathrm{l}}\right)T_+ = (1 + R)L - K(T_+ - T_{\mathrm{d}}) \tag{15}$$

where

$$R = \frac{i\omega(C_{\mathrm{p}} - C_{\mathrm{l}}) + K}{i\omega C_{\mathrm{l}} + S_+} \tag{16}$$

$$T_+ = \frac{T_{\mathrm{l}} + T_{\mathrm{p}}}{2} \tag{17}$$

$$S_+ = S_1 + S_2 \tag{18}$$

$$S_- = S_1 - S_2 \tag{19}$$

S_1 and S_2 are calculated from the thermal diffusion equation as explained in Appendix B. It is assumed that the heat capacity per unit length c, thermal conductivity κ and the thickness h of the sample satisfy the following condition:

$$\left(\sqrt{\frac{\omega c}{\kappa}h}\right)^2 \ll 1 \tag{20}$$

Then, S_+ and S_- are expressed by the following equations:

$$S_+ = \frac{2\kappa}{h} \tag{21}$$

$$S_- = \frac{i\omega ch}{2} \tag{22}$$

In most cases, C_{l} and C_{p} are of the same order with the heat capacity of the sample that is given by ch. Since the condition (20) can be rewritten as follows:

$$\omega\, ch \ll \frac{\kappa}{h} \tag{23}$$

Eq. (16) is approximated by the following equation:

$$R = \frac{K}{2\kappa/h} \tag{24}$$

If the sample is thin enough to satisfy

$$\frac{K}{2\kappa/h} \ll 1 \tag{25}$$

then, Eq. (15) becomes

$$i\omega(ch + C_{\mathrm{p}} + C_{\mathrm{l}})T_{+} = L - K(T_{+} - T_{\mathrm{d}}) \tag{26}$$

Eq. (26) is the same form with Eq. (7). Consequently, if the sample thickness satisfies the conditions (20) and (25) the sample, the lid and the pan can be regarded as one body of uniform temperature as assumed in the model 2. Besides, if the sample is thin enough to satisfy the condition (12) the model 1 can be used.

It should be noted that solution of the one-dimensional thermal diffusion equation for semi-infinite material shows that temperature in the area of a thickness sufficiently smaller than the decay distance given by the inverse of $\sqrt{\omega c/2\kappa}$ can be regarded as being uniform. This seems to suggest that the sample thickness, h should satisfy the condition $\sqrt{(\omega c/\kappa)}(h \ll 1)$. However, the condition (20) is more moderate than this condition. In the case of the solution for the semi-infinite material, the condition (20) allows linear temperature gradient in the sample. A sample, that does not satisfy the condition $\sqrt{(\omega c/\kappa)}(h \ll 1)$, could give meaningful results.

4. Frequency dependence

Results from model 2 are compared with experimental results obtained by LMDSC. Only the sample side was irradiated. This allows to set $L' = 0$. Frequency range investigated was from 0.1 to 1 Hz. In this frequency range, heat exchange between the sample and reference sides can be neglected [7], i.e. $M_1 = M_2 = M'_1 = M'_2 = 0$. Remembering $T_{\mathrm{b}} = 0$ for LMDSC we obtain the following equation from Eq. (10):

$$\frac{1}{\Delta T} = \frac{(i\omega C_{\mathrm{d}} + B_1 + K/Q) + i\omega C_{\mathrm{m}}(i\omega C_{\mathrm{s}} + K) - K^2}{QLK} \tag{27}$$

Since the measuring point of LMDSC is close to the "detector area" of the base plate, we use the Newton's law for the heat exchange between them. Eq. (9) and (A.15) (Appendix A) are replaced with the following equations:

$$i\omega C_{\mathrm{m}} T_{\mathrm{m}} = -K_{\mathrm{m}}(T_{\mathrm{m}} - T_{\mathrm{d}}) \tag{28}$$

$$Q = \left(1 + i\omega\frac{C_{\mathrm{m}}}{K_{\mathrm{m}}}\right)^{-1} \tag{29}$$

where K_{m} is the coefficient of the Newton's law. We assume that B_1 has the same form with S_1 of Eq. (B.4) (Appendix B).

$$B_1 = \frac{\kappa_{\mathrm{B}}}{h_{\mathrm{B}}}\left(1 + \frac{i\omega c_{\mathrm{B}} h_{\mathrm{B}}}{3\kappa_{\mathrm{B}}}\right) \equiv B_{1\mathrm{r}} + i\omega B_{1i} \tag{30}$$

where c_{B}, κ_{B} and h_{B} correspond to c, κ and h of Eq. (B.4), respectively. Substituting Eqs. (27) and (30) the following equations are deduced:

$$\begin{aligned} Re\left(\frac{KL}{\Delta T}\right) = -\omega^2\Bigg(&\left(C_{\mathrm{d}} + B_{1i} + C_{\mathrm{m}}\left(1 + \frac{K}{K_{\mathrm{m}}} + \frac{B_{1\mathrm{r}}}{K_{\mathrm{m}}}\right)\right)C_{\mathrm{s}} \\ &+ \frac{K}{K_{\mathrm{m}}}C_{\mathrm{m}}(C_{\mathrm{d}} + B_{1i})\Bigg) + B_{1\mathrm{r}}K \end{aligned} \tag{31}$$

$$\begin{aligned} \frac{1}{\omega}\mathrm{Im}\left(\frac{KL}{\Delta T}\right) = &-\omega^2\frac{(C_{\mathrm{d}} + B_{1i})C_{\mathrm{m}}C_{\mathrm{s}}}{K_{\mathrm{m}}} \\ &+ K^2\Bigg(\frac{C_{\mathrm{s}}}{K}\left(1 + \frac{B_{1\mathrm{r}}}{K}\right) + \frac{C_{\mathrm{m}}}{K_{\mathrm{m}}}\left(1 + \frac{B_{1\mathrm{r}}}{K}\right) \\ &+ \frac{C_{\mathrm{d}}}{K} + \frac{C_{\mathrm{m}}}{K} + \frac{B_{1i}}{K}\Bigg) \end{aligned} \tag{32}$$

Eqs. (31) and (32) show that $Re\,(KL/\Delta T)$ and $1/\omega\ \mathrm{Im}(KL/\Delta T)$ are linear to the square of the frequency. It can be seen from Eq. (32) that the value of $1/\omega\ \mathrm{Im}(KL/\Delta T)$ is independent of C_{s} at the frequency satisfying the following equation:

$$-\omega^2\frac{(C_{\mathrm{d}} + B_{1i})C_{\mathrm{m}}}{K_{\mathrm{m}}} + K + B_{1\mathrm{r}} = 0 \tag{33}$$

Fig. 3(a) and (b) show the graph of $Re\,(KL/\Delta L)$ and $1/\omega\ \mathrm{Im}(KL/\Delta L)$, respectively, plotted against square of the frequency. In Fig. 3, the magnitude of KL was set to be unity. The pans containing 0, 1 and 2 lids were used as the sample materials. Very small amount of grease was painted on the lids to reduce the thermal resistance. Straight lines could be fitted sufficiently well to the experimental results obtained from various heat capacities of the sample. In Fig. 3(b), the coincidence point where all lines meet can be clearly

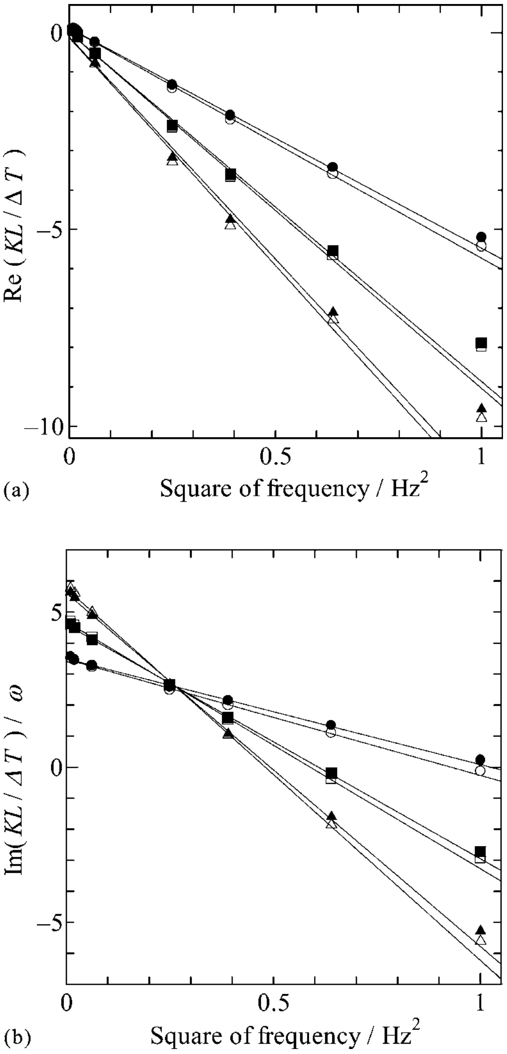

Fig. 3. Experimental results of Eqs. (31) and (32) are plotted against square of the frequency in (a) and (b), respectively. Modulation period was 1, 1.25, 1.6, 2, 4, 7 and 10 s. Circles, triangles and squares show the results from the pan containing 0, 1 and 2 lids, respectively. Measurement of the open symbols was made firstly. After pressing the lid lightly measurement of the solid symbols was made. Straight lines were fitted to the data excepting 1 Hz.

observed. The earlier results strongly support the applicability of the model 2 to LMDSC. At present, the same experiment can not be done using the commercial instruments because of two reasons. Firstly, the commercial instruments can not be operated at the high frequencies as this experiments. Secondly, temperature modulation only on the sample side can not be made. However, LMDSC was constructed using a commercial heat flux type DSC and the basic design of most of the commercial heat flux type DSC is similar to each other. It seems reasonable to consider that the model 2 will be applicable to the commercial type MTDSC when high frequency measurement becomes possible.

5. Data analysis based on the model 2

Two methods of data analysis based on Eq. (10) of the model 2 are presented. Same equations with these methods were used in data analysis of LMDSC [5,6] but those were deduced starting from simplified models and systematic explanation has not been given. In method 1, both the sample and reference sides are irradiated and in method 2 only the sample side is irradiated. In both the methods, only ΔT is used.

5.1. Method 1

Deviation from the symmetric thermal system is expressed by ε defined by the following equation:

$$\varepsilon \equiv \mu_{\rm L} L - \mu'_{\rm L} L' + \mu_{\rm b} T_{\rm b} \tag{34}$$

Eq. (10) is rewritten as

$$\Delta T - \frac{\varepsilon}{\xi} = \frac{((\lambda_{\rm L} L' + \lambda_{\rm b} T_{\rm b}) - \nu(\varepsilon/\xi))\Delta C}{\nu\Delta C + \xi} \tag{35}$$

ΔC can be calculated by the following equation:

$$\frac{1}{\Delta C_{\rm x}} = \alpha \frac{(1/\Delta T_{\rm x}) - (1/\Delta T_{\rm a})}{(1/\Delta T_{\rm b}) - (1/\Delta T_{\rm a})}\left(\frac{1}{\Delta C_{\rm b}} - \frac{1}{\Delta C_{\rm a}}\right) + \frac{1}{\Delta C_{\rm a}} \tag{36}$$

where

$$\alpha = \left(\frac{((1/\Delta T_{\rm x} - \varepsilon)/\xi) - ((1/\Delta T_{\rm a} - \varepsilon)/\xi)}{1/((\Delta T_{\rm b} - \varepsilon)/\xi) - ((1/\Delta T_{\rm a} - \varepsilon)/\xi}\right) \Big/ \left(\frac{(1/\Delta T_{\rm x}) - (1/\Delta T_{\rm a})}{(1/\Delta T_{\rm b}) - (1/\Delta T_{\rm a})}\right) \tag{37}$$

Subscripts x, a and b means the unknown sample and the standard samples a and b, respectively. Values of the correction factor α are calculated as shown in Table 1 assuming that $\Delta T_{\rm a} = 10$, $\Delta T_{\rm b} = 20$ and $\varepsilon/\xi = 1$. Difference from unity is less than a few

Table 1
Calculated values of the correction factor

ΔT_x	20	19	18	17	16	15	14	21	25
α	1	1.003	1.006	1.009	1.013	1.018	1.023	0.997	0.990

percent within the calculated values of ΔT_x. Results that are good enough for practical purposes can be obtained assuming that $\alpha = 1$.

5.2. Method 2

Deviation from the symmetric condition is not necessary to be considered in this model. The system is essentially asymmetric because only the sample side is irradiated. We put $L' = 0$ and $T_b = 0$ in Eq. (10).

$$\Delta T = \frac{\mu_L L}{v\,\Delta C + \xi'} \tag{38}$$

The following equation is obtained:

$$\Delta C = \frac{\mu_L L}{v}\frac{1}{\Delta T} - \frac{\xi'}{v} \tag{39}$$

Eq. (39) shows that $1/\Delta T$ plays a similar role to the conventional DSC signal. This proposes a convenient method to detect anomalous behavior of the heat capacity as can be done by the conventional DSC. Quantitative measurement can be done using the standard materials, a and b.

$$\Delta C_x = \frac{(1/\Delta T_x) - (1/\Delta T_a)}{(1/\Delta T_b) - (1/\Delta T_a)}(\Delta C_b - \Delta C_a) + \Delta C_a \tag{40}$$

Eq. (40) has an advantage of being free from the effects of asymmetry comparing with Eq. (36) but the method 2 is not the differential measurement.

6. Conclusions

Two models for the thermal system of MTDSC were studied. In the model 1 the sample, the lid, the pan and the “detector are of the base plate” were regarded as one body without temperature distribution. This model is suitable for the low frequency measurement. In the model 2, thermal resistance between the pan and the base plate and time lag between the temperature change at the detector and the measured temperature were taken into account. These two factors can not be neglected at high frequencies. In both the models, the effects of deviation from the symmetric thermal system was considered. Results from the model 1 showed that ΔC was proportional to $\Delta T/T_s$ as in the case of Wunderlich's equation only if deviation from the symmetric thermal system was negligible. Results from the model 2 showed that proportionality between ΔC and $\Delta T/T_m$ did not hold if deviation from the symmetric system was negligible. The upper limit of the sample thickness was calculated based on the model 2. It was found that the upper limit could be larger than the thickness of the area in the semi-infinite material where temperature gradient could be neglected. Frequency dependence measured by LMDSC was in good agreement with the results from the model 2. Two methods of data analysis that use only ΔT were proposed. These method were considered to be better than the method to use $\Delta T/T_m$ from the viewpoint of the signal-to-noise ratio.

Appendix A

The instrumental parameters appeared in Eqs. (10) and (11) are given as follows:

$$\lambda_L = -(PQ' - M_2Q)\frac{K'}{i\omega C_r + K'}i\omega \tag{A.1}$$

$$\lambda_b = -\left((PQ' - M_2Q) - (P'Q - M_2'Q') + \frac{K'}{i\omega C_r + K'}K'Q\right)B_2' i\omega \tag{A.2}$$

$$\mu_L = \left(P'Q - M_2'Q' - \frac{K'}{i\omega\,C_r + K'}K'Q\right)K \tag{A.3}$$

$$\mu_L' = \left(PQ' - M_2Q - \frac{K}{i\omega C_r + K}KQ'\right)\frac{i\omega C_r + K}{i\omega C_r + K'}K' \tag{A.4}$$

$$\begin{aligned}\mu_b = &\left(\left(P'Q - M_2'Q' - \frac{K'}{i\omega C_r + K'}K'Q\right)B_2\right.\\ &\left.- \left(PQ' - M_2Q - \frac{K}{i\omega C_r + K}KQ'\right)B_2'\right)\\ &\times (i\omega C_r + K)\end{aligned} \tag{A.5}$$

$$v = \left(\left(P' - \frac{K'}{i\omega C_r + K'}K'\right)P - M_2M_2'\right)i\omega \tag{A.6}$$

$$\begin{aligned}\xi = &(i\omega\, C_r + K)\left(\left(P' - \frac{K'}{i\omega\, C_r + K'}K'\right)\right.\\ &\left.\times \left(P - \frac{K}{i\omega\, C_r + K}K\right) - M_2M_2'\right)\end{aligned} \tag{A.7}$$

$$\eta_L = \left(M_2\frac{K'}{i\omega C_r + K'}\right)Qi\omega \tag{A.8}$$

$$\eta_b = \left(P' - \frac{K'}{i\omega\, C_r + K'}K'\right)B_2Q\, i\omega + M_2B_2'Q\ \ i\omega \tag{A.9}$$

$$\zeta_L = \left(P' - \frac{K'}{i\omega\, C_r + K'}K'\right)KQ \tag{A.10}$$

$$\zeta_L' = (i\omega C_r + K)\frac{K'}{i\omega C_r + K'}M_2Q \tag{A.11}$$

$$\begin{aligned}\zeta_b = &\left(\left(P' - \frac{K'}{i\omega C_r + K'}K'\right)B_2 + M_2B_2'\right)\\ &\times (i\omega C_r + K)Q\end{aligned} \tag{A.12}$$

In the previous equations, the following symbols are used:

$$P = i\omega C_d + M_1 + B_1 + K + D_{d1} - D_{d2}Q \tag{A.13}$$

$$P' = i\omega C_d' + M_1' + B_1' + K' + D_{d1}' - D_{d2}'Q' \tag{A.14}$$

$$Q = \frac{D_{m2}}{\mathrm{i}\omega C_m + D_{m1}} \tag{A.15}$$

Appendix B

The coefficients S_1, and S_2 in Eqs. (13) and (14) are calculated from the thermal diffusion equation assuming a uniform material. We consider only the temperature change in the thickness direction of the sample. Following the ordinary method we obtain the following solution:

$$\begin{aligned}T(x) = &\frac{\exp(\sqrt{(i\omega c/\kappa)h})T_l - T_p}{\exp(\sqrt{(i\omega c/\kappa)}h) - \exp(-\sqrt{(i\omega c/\kappa)}h)}\\ &\times \exp\left(-\sqrt{\frac{i\omega c}{\kappa}}x\right)\\ &+\frac{-\exp(-\sqrt{(i\omega c/\kappa)}h)T_l + T_p}{\exp(\sqrt{(i\omega c/\kappa)}h) - \exp(-\sqrt{(i\omega c/\kappa)}h)}\\ &\times \exp\left(\sqrt{\frac{i\omega c}{\kappa}}x\right)\end{aligned} \tag{B.1}$$

where x is the distance measured from the top surface of the sample. Time dependence is omitted in Eq. (B.1). Eq. (B.1) satisfies the boundary conditions, $T(0) = T_l$ and $T(h) = T_p$. Since S_1T_l and $-S_2T_p$ give the heat flow into the sample at $x = 0$ accompanying changes in T_l and T_p, respectively, S_1 and S_2 are given by the following equations:

$$\begin{aligned}S_1 &= -\frac{\kappa}{T_l}\frac{\mathrm{d}T(x = 0, T_p = 0)}{\mathrm{d}x}\\ &= \sqrt{i\omega c\kappa}\frac{\exp\left(\sqrt{(i\omega c/\kappa)}h\right) + \exp\left(-\sqrt{(i\omega c/\kappa)}h\right)}{\exp\left(\sqrt{(i\omega c/\kappa)}h\right) - \exp\left(-\sqrt{(i\omega c/\kappa)}h\right)}\end{aligned} \tag{B.2}$$

$$\begin{aligned}S_2 &= \frac{\kappa}{T_p}\frac{\mathrm{d}T(x = 0, T_l = 0)}{\mathrm{d}x}\\ &= \sqrt{i\omega c\kappa}\frac{2}{\exp(\sqrt{(i\omega c/\kappa)}h) - \exp(-\sqrt{(i\omega c/\kappa)}h)}\end{aligned} \tag{B.3}$$

To the second-order approximation for $\sqrt{i\omega\, c/\kappa}$ the following equations can be obtained from Eqs. (B.2) and (B.3):

$$S_1 = \frac{\kappa}{h}\left(1 + \frac{1}{3}\frac{i\omega ch^2}{\kappa}\right) \tag{B.4}$$

$$S_2 = \frac{\kappa}{h}\left(1 - \frac{1}{6}\frac{i\omega ch^2}{\kappa}\right) \tag{B.5}$$

$$S_1 - S_2 = \frac{i\omega\, ch}{2}\left(1 - \frac{1}{12}\frac{i\omega ch^2}{\kappa}\right) \tag{B.6}$$

References

[1] B. Wunderlich, Y. Jin, A. Boller, Thermochim. Acta 238 (1994) 277.

[2] I. Hatta, J. Appl. Phys. 33 (1994) L686.

[3] M. Nishikawa, Y. Saruyama, Thermochim. Acta 267 (1995) 75.

[4] Y. Saruyama, J. Therm. Anal. 54 (1998) 687.

[5] Y. Saruyama, Thermochim. Acta 283 (1996) 157.

[6] Y. Saruyama, Thermochim. Acta 304/305 (1997) 171.

[7] Y. Saruyama, J. Therm. Anal. Calc. 59 (2000) 271.